

A return mapping algorithm for plane stress and degenerated shell plasticity

Z. Liu[†] and F.G.A. Al-Bermani[‡]

Department of Civil Engineering, University of Queensland, QLD 4072, Australia

Abstract. A numerical algorithm for plane stress and shell elasto-plasticity is presented in this paper. The proposed strain decomposition (SD) algorithm is an elastic predictor/plastic corrector algorithm, and in the context of operator splitting, is a return mapping algorithm. However, it differs significantly from other return mapping algorithms in that only the necessary response functions are used without invoking their gradients, and the stress increment is updated only at the end of the time step. This makes the proposed SD algorithm more suitable for materials with complex yield surfaces and will guard against error accumulation during the time step. Comparative analyses of structural systems using the proposed strain decomposition (SD) algorithm and the iterative radial return (IRR) algorithm are presented. The results demonstrate the accuracy and usefulness of the proposed algorithm.

Key words: algorithm; finite element; numerical technique; plane stress; plasticity; shell.

1. Introduction

The elasto-plastic analysis of shell structures has drawn considerable attention in the last few years because shell structures generally exhibit a highly nonlinear response. Several numerical algorithms have been developed for plane stress and shell elasto-plasticity. These algorithms can be viewed in a 'stress return mapping' context whereby a procedure is provided to bring the stress point back to the yield surface. As shown by Ortiz and Popov (1985), these procedures are only approximate algorithms. They are used to integrate rate constitutive equations over a time step and represent a generalized trapezoidal or mid-point rule.

The plane stress condition is not a trivial constraint on a return algorithm since some properties in general stress space may be lost (e.g. the constant curvature of the Von Mises yield contour in the Π -plane). This may result in a dramatic increase in computation time. Several algorithms have evolved to satisfy this constraint. The iterative radial return (IRR) algorithm by Hallquist and Benson (1986) uses an iterative correction for the three-dimensional radial return algorithm to satisfy the constraint of zero normal stress for plane stress. The plane stress projection algorithm proposed by Simo and Taylor (1986) is based on projecting the three-dimensional equations of elasto-plasticity into a plane stress subspace and requires solution of a nonlinear scalar algebraic equation.

In this paper a new algorithm is proposed. This algorithm exploits three principals of plasticity: (i) constitutive laws have an additive structure, (ii) the plasticity consistency condition is satisfied, and (iii) no volume change is associated with plastic strain. Based on these principals, the strain

[†] Research Student

[‡] Senior Lecturer

tensor is decomposed into elastic and plastic components using a bisection method. The stresses are then updated at the end of each time step when the correct strain decomposition is achieved. This approach does not use the gradient of the response functions and hence can be extended easily to materials with complex yield surfaces.

Although an assessment of numerical algorithms for plane stress and shell plasticity based on iso-error maps shows that the iterative radial return (IRR) algorithm is more efficient and accurate than others (Whirley, Hallquist and Goudreau 1989), few practical applications are available to demonstrate the behaviour of the algorithm in a complex loading situation. In this paper, the behaviour of the proposed strain decomposition (SD) algorithm is compared with that of the IRR algorithm. Several examples involving simple structural systems are presented and used for comparison. The comparisons are restricted to Von Mises solids only, although the present SD algorithm can be extended to other materials and hardening rules.

2. Preliminaries

The additive structure of the elasto-plastic constitutive law implies that

$$\varepsilon_{ij} = \varepsilon_{ij}^e + \varepsilon_{ij}^p \quad (1)$$

where ε_{ij} is the strain tensor. The superscripts e and p refer, respectively, to the elastic and the plastic components. The stress tensor σ_{ij} is related to the elastic strains through the material tensor D_{ijkl} via

$$\sigma_{ij} = D_{ijkl} \varepsilon_{kl}^e \quad (2)$$

Eq. (2) can be expressed as

$$\sigma_{ij} = 2G \varepsilon_{ij}^e - P \delta_{ij} \quad (3)$$

in which

$$P = -\lambda \varepsilon_{kk}^e \quad (4)$$

where G and λ are Lamé's constants and δ_{ij} the Kronecker delta.

Since the volume is unchanged during plastic deformation, the plastic strain tensor must satisfy the following condition, i.e.,

$$\varepsilon_{kk}^p = 0 \quad (5)$$

and the plastic consistency condition implies that

$$\dot{\phi} = 0 \quad (6)$$

where ϕ is a yield function.

Eqs. (1)-(6) represent all the necessary equations needed for the proposed algorithm.

3. Plastic return strategy

If the stress state σ_n is known at time t_n then using Eqs. (1)-(2) the stress state σ_{n+1} at time t_{n+1} can be written as (the index notations are dropped for clarity)

$$\sigma_{n+1} = \sigma_{n+1}^{Tr} - D : \Delta \varepsilon^p \quad (7)$$

where the symbol $(:)$ signifies doubly contracted tensor product and D is the tangential stiffness tensor of the material. The elastic predictor σ_{n+1}^{Tr} is given by

$$\sigma_{n+1}^{Tr} = \sigma_n + D : (\varepsilon_{n+1} - \varepsilon_n) \quad (8)$$

The integration of Eq. (7) can be conceived as a generalized trapezoidal or mid-point rule (Ortiz and Popov 1985). For a plane stress condition, the through-thickness stress component should be zero (i.e., $\sigma_{33}=0$). In the iterative radial return (IRR) algorithm (Hallquist and Benson 1986), secant iterations are performed to satisfy this condition.

In the present strain decomposition (SD) approach, an iterative bisection procedure is performed in which the constraint condition of plane stress ($\sigma_{33}=0$) is implicitly satisfied. This algorithm represents a one step backward Euler scheme.

Considering the plane stress condition and using Eq. (3),

$$\Delta \varepsilon_{33}^e = -\frac{\lambda}{\lambda + 2G} (\Delta \varepsilon_{11}^e + \Delta \varepsilon_{22}^e) \quad (9)$$

while the plastic part of $\Delta \varepsilon_{33}$ can be obtained from Eq. (5),

$$\Delta \varepsilon_{33}^p = -\Delta \varepsilon_{11}^p - \Delta \varepsilon_{22}^p \quad (10)$$

Assuming that for every strain component other than ε_{33}

$$\Delta \varepsilon_{ij}^e = \alpha \Delta \varepsilon_{ij} \quad (i \neq 3 \text{ and } j \neq 3) \quad (11)$$

and using Eq. (1), the following may be obtained:

$$\Delta \varepsilon_{ij}^p = (1 - \alpha) \Delta \varepsilon_{ij} \quad (i \neq 3 \text{ and } j \neq 3) \quad (12)$$

where α is an algorithmic parameter ($0 \leq \alpha \leq 1$). Elastic behaviour is described by setting $\alpha = 1$, while fully plastic behaviour is described using $\alpha = 0$.

Substituting Eq. (11) into (9) gives

$$\Delta \varepsilon_{33}^e = -\frac{\lambda}{\lambda + 2G} \alpha (\Delta \varepsilon_{11} + \Delta \varepsilon_{22}) \quad (13)$$

and substituting Eq. (12) into (10) gives

$$\Delta \varepsilon_{33}^p = -(1 - \alpha) (\Delta \varepsilon_{11} + \Delta \varepsilon_{22}) \quad (14)$$

The through-thickness strain may be obtained by adding Eqs. (13) and (14)

$$\Delta \varepsilon_{33} = \left[\alpha \left(1 - \frac{\lambda}{\lambda + 2G} \right) - 1 \right] (\Delta \varepsilon_{11} + \Delta \varepsilon_{22}) \quad (15)$$

Substituting Eqs. (11) and (13) into (4) gives

$$\Delta P = -\frac{2G\lambda}{\lambda + 2G} \alpha (\Delta \varepsilon_{11} + \Delta \varepsilon_{22}) \quad (16)$$

and any stress increment (other than $\Delta \sigma_{33}$) can be obtained from substituting Eqs. (11) and (16) into Eq. (3)

$$\Delta \sigma_{ij} = 2G \alpha \Delta \varepsilon_{ij} - \Delta P \delta_{ij} \quad (i \neq 3 \text{ and } j \neq 3) \quad (17)$$

The through-thickness stress increment may be obtained from Eq. (3) and (16)

$$\Delta \sigma_{33} = 2G \Delta \varepsilon_{33}^e + \frac{2G\lambda}{\lambda + 2G} \alpha (\Delta \varepsilon_{11} + \Delta \varepsilon_{22}) \quad (18)$$

Substituting Eq. (13) into (18), gives

$$\Delta \sigma_{33} = 0 \quad (19)$$

Using Eqs.(17), (7) and (8),

$${}_i \sigma_{n+1} = \sigma_n + {}_i \Delta \sigma \quad (20)$$

with $(\sigma_{33})_{n+1} = 0$. The left subscript i in Eq. (20) refers to the number of the iteration. The bisection method is used to evaluate the algorithmic parameter α such that the consistency condition is satisfied, i.e.,

$$\phi({}_i \sigma_{n+1}) = 0 \quad (21)$$

Pseudo-code of the proposed SD algorithm is shown in Table 1. The procedure may be applied to any general yield surfaces.

Table 1 Pseudo code of proposed strain decomposition (SD) algorithm

-
- (1) Using the displacement increment Δu , calculate the strain increment
 $\Delta \varepsilon = [B] \Delta u$
 - (2) Elastic loading
 ${}_1 \alpha = 1$
Determine ${}_1 \sigma_{n+1}^{Tr}$ using ${}_1 \alpha$ and Eqs. (16)-(20)
Check Eq. (21)
If $\phi \leq tol$ goto Step 5 (elastic loading)
If $\phi > tol$ goto Step 3
 - (3) Fully plastic loading
 ${}_2 \alpha = 0$
Determine ${}_2 \sigma_{n+1}^{Tr}$ using ${}_2 \alpha$ and Eqs. (16)-(20)
Check Eq. (21)
If $|\phi| < tol$ goto Step 5 (fully plastic strain)
If $\phi < -tol$ goto Step 4
 - (4) Strain decomposition
 ${}_i \alpha = ({}_1 \alpha + {}_2 \alpha) / 2$
Determine ${}_i \sigma_{n+1}^{Tr}$ using ${}_i \alpha$ and Eqs. (16)-(20)
Check Eq. (21)
If $|\phi| \leq tol$ goto Step 5
If $\phi < -tol \rightarrow {}_2 \alpha = {}_i \alpha$ repeat Step 4
If $\phi > tol \rightarrow {}_1 \alpha = {}_i \alpha$ repeat Step 4
 - (5) Update stress components using recent value of ${}_i \alpha$
 $\sigma_{n+1} = {}_i \sigma_{n+1}^{Tr}$
-

Note: tol = a specified tolerance

4. Numerical examples

A number of examples are presented in this section to demonstrate the capabilities of the strain decomposition (SD) algorithm. The results obtained using the algorithm are compared

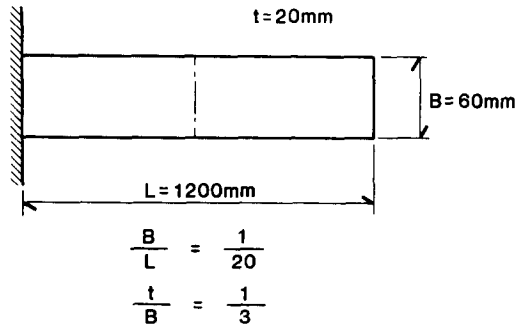


Fig. 1 Finite element discretization of a thin-plate cantilever.

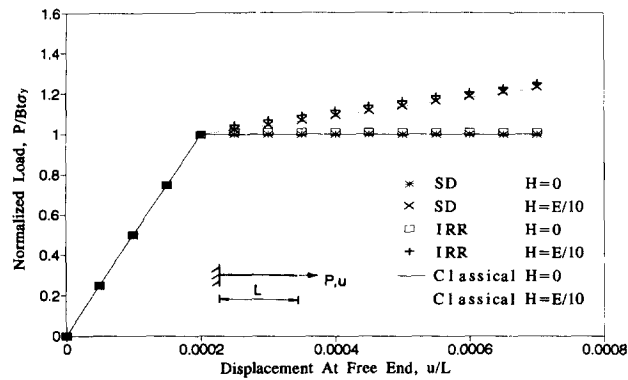


Fig. 2 Load-deflection curves for thin-plate cantilever under tension.

with those obtained using the iterative radial return (IRR) algorithm (Hallquist and Benson 1986) and with classical plasticity solutions or experimental results. Both the SD and IRR are implemented in a finite element program 'SHELL'. This program, written in "C", is based on an updated Lagrangian formulation using a twelve-node (5 dof per node) degenerated shell element ($3 \times 3 \times 3$ Gauss points), assuming a Von Mises isotropic material model and employing a displacement control solution strategy.

In the first three examples, a thin plate with a length L , width B , thickness t , yield stress σ_y , Poisson's ratio $\nu=0.3$, elastic modulus E and a hardening parameter of either $H=E/10$ or $H=0$ (i.e., elastic-perfectly plastic) has been used. The ratios B/L and t/B are taken as $1/20$ and $1/3$, respectively.

4.1. A cantilever plate under in-plane tension

A thin cantilever plate subjected to in-plane tension is shown in Fig. 1. The plate has been modelled using two elements. The axial displacement at the cantilever tip obtained using the proposed SD algorithm has been plotted against the applied load in Fig. 2, together with the results obtained using the IRR algorithm and the classical plasticity solution. It can be seen from Fig. 2 that the results predicted by both the SD and the IRR algorithms are in good agreement with the classical plasticity solutions for cases either with hardening ($H=E/10$) or without hardening ($H=0$).

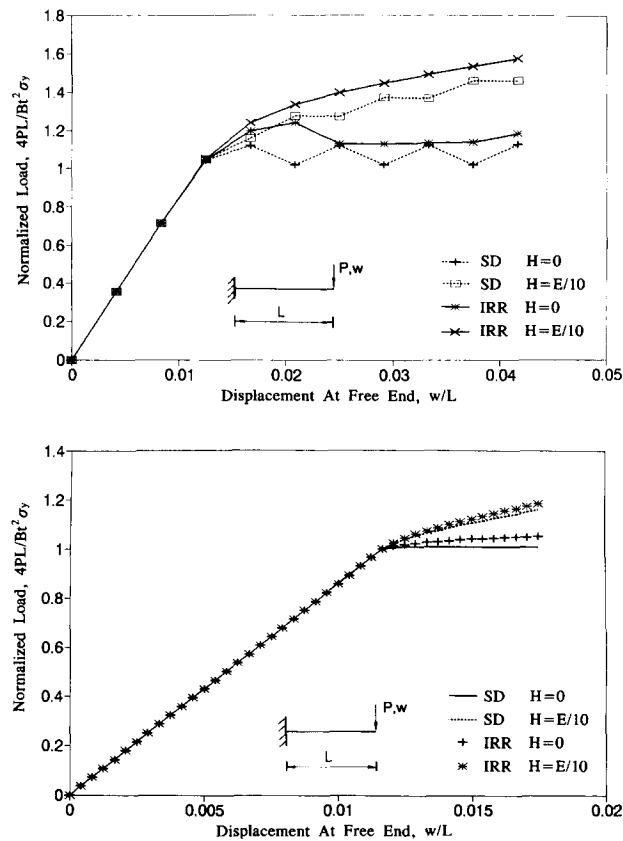


Fig. 3 Load-deflection curves for thin-plate cantilever under shear; (a) using a large displacement increment, (b) using a small displacement increment.

4.2. A cantilever plate under transverse loading

In order to test the proposed algorithm when the shear effect is predominant, the same cantilever plate used in the previous example has been analysed under the effect of a transverse load. The transverse displacements at the cantilever tip have been plotted against the applied load in Fig. 3. Load-deflection curves using both the SD and the IRR algorithms are shown in Figs. 3(a) and (b). In Fig. 3(a), a relatively large displacement increment ($\Delta w/L = 4.166 \times 10^{-3}$) has been used, while in Fig. 3(b) a small displacement increment ($\Delta w/L = 4.166 \times 10^{-4}$) has been used. It can be seen from these figures that the IRR results tend to overestimate the cantilever capacity when large or small displacement increments are used. Results using the SD algorithm converge exactly to the correct solution when a small displacement increment is specified but results fluctuate about the correct solution when large displacement increments are used. A similar conclusion may be drawn for the cases with and without hardening.

4.3. Bending of clamped plate

To investigate the performance of the SD algorithm when both flexural and membrane effects exist, a thin plate clamped on two opposite sides and free on the other two sides (see Fig.

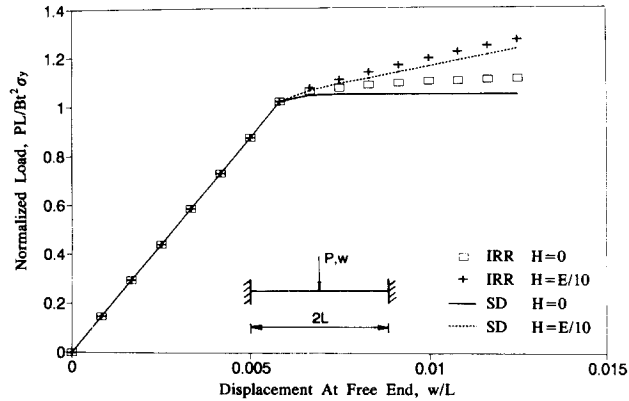


Fig. 4 Load-deflection curves for clamped thin plate.

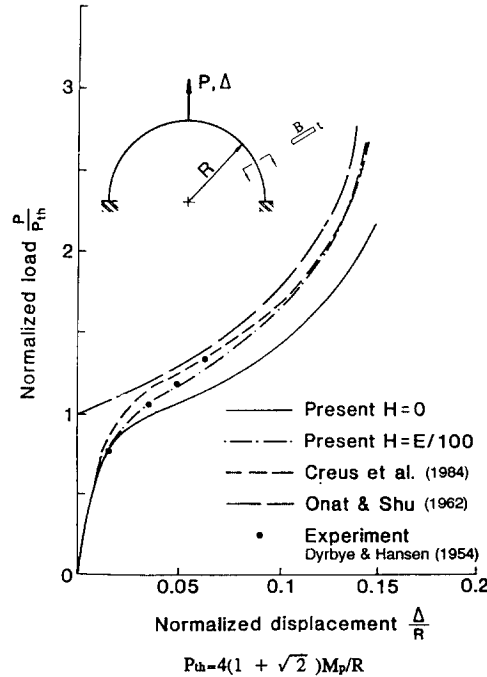


Fig. 5 Load-deflection curves for semicircular arch.

4) has been analysed. Due to symmetry, only one-half of the plate has been analysed, using two elements. The load-deflection curves for the out-of-plane displacement at the plate centre are plotted in Fig. 4. It can be seen that the SD algorithm yields results which are more accurate than those using the IRR algorithm.

4.4. A semicircular arch under a concentrated load

Fig. (5) shows a semicircular arch with rectangular section clamped at both ends and subjected to a concentrated upward load at the apex. This problem was solved analytically by Onat and

Shu (1962) and numerically by Creus, *et al.* (1984). Experimental results were also obtained by Dyrbye and Hansen (1954).

In the present analysis nine elements were used to model the arch. Both elastic-perfectly plastic and linear hardening with $H=E/100$ models are used. The present results are plotted in Fig. (5) together with available experimental and analytical results. It is seen that the present results are in good agreement with the experimental and analytical results particularly when the hardening is introduced.

5. Conclusions

A numerical return mapping algorithm for plane stress and shell elasto-plasticity has been presented. This algorithm is based on strain decomposition (SD) and utilizes the necessary response functions without their gradients. The stress increment is updated only at the end of the time step, preventing error accumulation during the step.

Numerical evaluations have been presented to demonstrate the accuracy of the proposed algorithm. The performance of the SD algorithm has been compared with the iterative radial return (IRR) algorithm and the results from both these algorithms have been checked against available analytical or experimental results. The examples reveal that the proposed SD algorithm yields accurate results.

Acknowledgements

The authors wish to thank Dr. F. Gatto of BHP Engineering Ltd. for proof-reading the manuscript.

References

- Creus, G. J., Torres, P. L. and Gorehs, A. G. (1984), "Elastoplastic frame analysis with generalized yield function and finite displacements", *Comp. & Struct.*, **18**(5), 925-929.
- Dyrbye, C. and Hansen, L. (1954), "Studies on the load carrying capacities of steel structures", Technical University of Denmark, Bulletin No.3.
- Hallquist, J. O. and Benson, D.J. (1986), "Finite element methods for plate and shell structures", *Element Technology* **1**, Hughes, T. J. R. and Hinton, E. Editors, Pineridge Press International, Swansea, 394-431.
- Onat, E. T. and Shu, L. S. (1962), "Finite deformation of a rigid perfectly plastic arch", *J. Applied Mech., Trans. ASME*, 549-553.
- Ortiz, M. and Popov, E. P. (1985), "Accuracy and Stability of integration algorithms for elastoplastic constitutive relations", *Int. J. Num. Meth. Engng.*, **21**, 1561-1576.
- Simo, J. C. and Taylor, R. L. (1986), "A return mapping algorithm for plane stress elastoplasticity", *Int. J. Num. Math. Engng.*, **22**, 649-670.
- Whirley, R. G., Hallquist, J. O. and Goudreau, G. L. (1989), "An assessment of numerical algorithm for plane stress and shell elastoplasticity on supercomputers", *Eng. Comput.*, **6**, 116-126.